



Antibacterial Activity of Chitosan Nanoparticles Loaded with *Syzygium aromaticum* Extract against *Klebsiella pneumonia*

Hussein A. Shaghati , Emad H. Jassim

Institute of Genetic Engineering and Biotechnology for Postgraduate Studies, University of Baghdad

Received: June 22, 2022/ Accepted: September 5, 2022 /Published: June 4, 2023

Abstract: The present study aims to describe the antibacterial activity of chitosan nanoparticles loaded with *Syzygium aromaticum* extract against MDR *Klebsiella pneumonia*. 50 isolates of *K. pneumoniae* were collected from patients with urinary tract infections. The isolates were diagnosed as *Klebsiella pneumoniae* by classical biochemical tests and PCR technique using *16S rRNA* gene as a diagnostic gene and gel electrophoresis. The sensitivity of bacteria to antibiotics was tested using the Kerby-Bauer method. Measuring the diameters of inhibition and testing the effectiveness of the chitosan nanoparticles prepared in a previous study using spread plate method and counting the colonies growth. It was concluded to demonstrate that the chitosan nanoparticles loaded with *Syzygium aromaticum* extract have good antibacterial efficacy against MDR *Klebsiella pneumonia*.

Keywords: Chitosan nanoparticles, *Klebsiella pneumonia*, *Syzygium aromaticum* MDR, *16S rRNA*.

Corresponding author: (Email: hussein.ali1300a@ige.uobaghdad.edu.iq).

Introduction

Because of the increasing resistance to antibiotics by pathogenic microorganisms, it has become necessary to search for a novel source of antibiotics that are natural, safe, cheap, and effective against pathogenic microorganisms. Nanotechnology give great attention in recent years due to its physiological properties Its specific size, shape, and structure also influence its reactivity, toughness, and other characteristics (1). The dried flower buds of *Syzygium aromaticum* (*S. aromaticum*) belong to Myrtaceae Family, sometimes known as clove, are a traditional spice used for food preservation and have a variety of therapeutic characteristics (2). Clove is a rich source of phenolic chemicals such as flavonoids, hydroxybenzoic acids, hydroxycinnamic acids, and hydroxyphenyl propene. Eugenol is the primary bioactive chemical found in

clove, with quantities ranging from 9 381.70 to 14 650.00 mg per 100 g of fresh plant material (3). Flavonoids, phenols, citric acid, ascorbic acid, polyphenolic, terpenes, alkaloids, and reductase are examples of bioactive compounds found in plants that serve as reducing agents. Plant-mediated nanoparticle synthesis is a particularly promising subject of nanotechnology since the plant acts as both a reducing and capping agent (4). Many plant-derived extracts are featured here due to their potential as environmentally safe scavenging free radicals, microbicidal agents, or antibiotic alternatives, considering that the majority of the latter have resulted in bacterial resistance due to overuse and/or underuse. They can have greater and longer-lasting bioactivity when encapsulated in small-scaled particles (5). The antibacterial effect of Chitosan nanoparticles is most likely due to

interactions with the bacterial cell wall or cell membrane. Various Process Theories have been proposed in an attempt to explain this process (6). The most often stated Chitosan NPs antibacterial action mechanism is the electrostatic link between the positively charged amino groups of glucosamine

and the negatively charged cell membranes of bacteria (7). This interaction produces broad alterations to the surface of the cell, resulting in a change in membrane permeability, which causes osmotic imbalance and intracellular substance efflux, ultimately leading to cell death figure(1) (5,8).

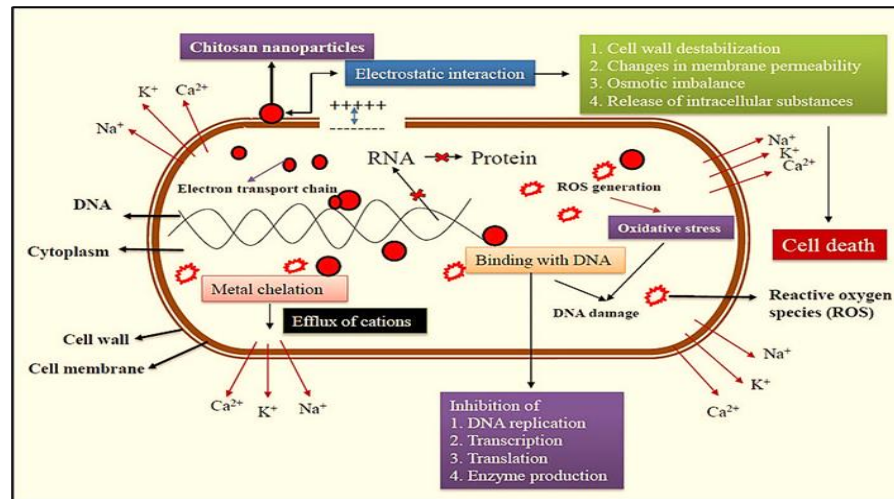


Figure (1): Antibacterial mechanisms of chitosan nanoparticles (5)

The *K. pneumoniae* is a clinically important bacterium it is a prevalent source of diseases associated with health care environments, such as pneumonia, urinary tract infections UTI, and bloodstream infections (9). It is a gram-negative, encapsulated, gas-producing, non-motile, lactose-fermenting, facultatively anaerobic bacteria with a rod-like form under the microscope. It is a typical bacterium that lives in the mouth and gut and belongs to the Enterobacteriaceae family. When *K. pneumoniae* is moved somewhere else, it becomes harmful (10).

Materials and methods

Bacterial isolates

Fifty previously identified *K. pneumoniae* isolates from patients suffering from urinary tract infections were obtained from al-Karama and ghazi al-Hariri hospitals in Baghdad During the period from December 2021

until February 2022. The isolates were cultured on CHROMagar, blood agar, and MacConkey agar and incubated at 37°C for 24 h. Tests including morphological properties, gram stain procedures, and standard biochemical tests were used.

Biochemical tests

Classical biochemical tests were performed on the isolates to confirm their identification. Which were: Gram stain, Catalase production, Oxidase test, Indole production, Urease production, Lactose fermentation, Motility test, and microscopic shape. All the tests were performed as per (11,12).

Genotypic identification

DNA extraction of bacteria

Bacterial DNA was extracted from all isolates using Favor Prep Blood/ Cultured Cells Genomic DNA Extraction Mini Kit/Korea which was intended to extract DNA from Gram-negative bacteria using a 1ml nutrient

broth sample in a 1.5 microcentrifuge tube the extract was stored in a deep freeze for further use.

Identification gene selection

In this study, a traditional polymerase chain reaction PCR test was used to identify the *16S rRNA* gene for identifying the *K. pneumoniae* subspecies. *16srRNA* primer (1419bp) was provided by Favorgen, Korea 27F (5'-AGAGTTTGATCCTGGCTCAG-3') and 1392R (5'GGTTACCTTGTTACGACTT-3'). PCR products were visualized on a 1% agarose gel stained with a red safe(13).

Preparation of primers

The primer was in lyophilized form. As indicated by the supplier, it consists of i-Taq™ DNA polymerase 5U/μl 2.5U, dNTPs 2.5mM each, Reaction Buffer 10x, and Gel Loading buffer 1x. They were dissolved in sterile nuclease-free water to achieve a final concentration of 100 Picomole/μl as a stock solution. Pipetting 10 μl from the stock solution into 90 μl of nuclease-free water to obtain a final concentration of 10 pmol/μl was used as a work solution, and then kept in a deep freezer until ready to use.

Amplification reaction

Using 25μL of PCR reaction, 1.5 μl DNA template amplified using 5 μl of Taq PCR PreMix and 1 μl of each primer 10 pmol/μL of the gene, up to the final volume of 25 μl with nucleases free water. The extracted DNA, primers, and PCR premix were thawed at 4°C, vortexed, and centrifuged briefly to bring the contents to the bottom of the tubes. Optimization of the polymerase chain reaction was accomplished after several trials. The negative control contained all material except DNA, so nuclease-free water was added instead of template DNA. PCR programs were set on Thermal-cycler Applied BioSystem/ USA.

The cycling conditions of the *16S rRNA* gene

The program was performed for amplification by PCR which was designed in the current study, initial denaturation 95°C for 5 min 1 cycle, Denaturation 95 °C for 45 sec, annealing at 56 °C for 45 sec, Extension at 72 °C for 1 min, these three steps repeated for 35 cycles and finally Final extension at 72 °C for 5 min 1cycle.

Agarose gel-electrophoresis of the PCR product

All products were tested by agarose gel electrophoresis. 1.5g agarose gel with 100ml 1x TBE stained with red stain 3 μl in the wells of the gel, 8μl of PCR products were put in each well. To detect PCR product size, a DNA ladder Kapa /USA 100bp was performed simultaneously with an electrophoretic run. UV transilluminator documentation system was used to see DNA bands. The gel was covered with TBE, the tank was closed, and electrophoreses were run for 1 hour at 5 volt/cm of the gel. After that, the agarose gel was taken out of the tank and photographed using a UV transilluminator (14).

Antibiotic susceptibility assays

Antibiotics were chosen based on the Institute of Clinical Standards and Laboratories' recommendations CLSI 2021 the discs were Ceftriaxone, Ciprofloxacin, Nalidixic acid, Gentamicin, Imipenem, Meropenem, Amoxicillin/ Clavulanic, Tobramycin, Cefotaxime, Ceftazidime, Nitrofurantoin, Trimethoprim, and Tetracycline. Antibacterial susceptibility testing was prepared according to the Kirby-Bauer method that was described by (15). briefly, 1-2 colonies were transferred to 3 mL of normal saline from an overnight nutrient agar plate culture. the turbidity was adjusted to 0.5

McFarland A sterile cotton swab immersed into the bacterial suspension was inoculated into Muller Hinton agar plates, Different antibiotic discs were used, put on the surface of the medium with sterilized forceps, and later the plates were inverted and incubated at 37°C for 18-24 hours. The resulting zones of inhibition were measured and compared with the breakpoints of CLSI 2021. By comparing the isolate to conventional inhibition zones, the isolate was classified as sensitive, intermediate, or resistant to a certain antibiotic according to (15).

Preparation of *S. aromaticum* extract

The air-dried powdered plant material (150 g from the sample) was extracted for 8 hours under Soxhlet on a water bath with the solvent aqueous methanol (methanol 80 %: water 20 % v/v) 500 ml. The extracts were concentrated and dried using a rotary evaporator (16).

Gas-chromatography-mass spectrometry analysis (GC-MS)

Chemical components of the samples were identified by an Agilent (7820A) GC Mass Spectrometer, analytical Column: Agilent HP-5ms Ultra inlet (30 m length x 250 µm diameter x 0.25 µm inside diameter) Injection volume 1µl, Pressure 11.933 psi, GC Inlet Line Temperature: 250 °C, Aux heaters Temperature 310 °C, Carrier Gas: He 99.99%, Injector Temperature: 250 °C Scan Range: m/z 50-500, Injection Type: Splitless (17).

Preparation of Chitosan/*S. aromaticum* Nanoparticles

Chitosan/ *S. aromaticum* solution was prepared according to (18). Briefly, Chitosan and 5% *S. aromaticum* extract were combined in equimolar ratios, condensation process was carried out in the presence of xylene using the Dean-Stark (Clevenger) apparatus until the theoretical quantity of water was

separated. Washing several times with methanol, hot distilled water, and ethanol, then dried in an electric oven at 50°C. The Chitosan NPs loaded *S. aromaticum* Extract were produced utilizing an ionic gelation process including Tripolyphosphate TPP and a chitosan-*S. aromaticum* extract adduct by dissolving 5 mg/ml of the chitosan-plant adduct in 1% w/v acetic acid solution, the pH value is adjusted to 7, stirring until the solution is clear then, TPP solution was added to the solution with ratios 1:2.5 (w/w), with continuous stirring at ambient temperature for 6h(19).

Characterization of chitosan NPs loaded *S. aromaticum* extract

The characterization of Chitosan NPs loaded *S. aromaticum* Extract achieved using UV-vis, FTIR, XRD, AFM, and SEM. in a previous study conducted by the same authors.

Spread plate method (SPM)

Mueller Hinton agar MHA is put onto several sterile Petri plates and allowed to solidify. Before using the plates, wait for a while to dry. As with the pour plate procedure. Bacterial suspension of moderate turbidity was prepared by picking 1-2 isolated colonies of *K. pneumoniae* from the original culture and introducing them into a test tube containing 4 ml of normal saline. It was compared to the standard turbidity solution the McFarland value which approximately equals 1.5×10^8 CFU/ml. The treatments with different concentrations of 100%, 50%, 25%, 12.5%, 6.25%, and 3.12% of *S. aromaticum* Extract loaded Chitosan NPs solution mixed with bacterial suspension, in addition to bacterial control (without treatment), pipette 100µl quantities of each dilution over the surface of each of the three plates. An ethanol-flamed glass spreader is then used to disseminate the sample

throughout the plate's surface. The plates are incubated for 24h at 37 °C in aerobic conditions and the number of colonies that form is counted in the same way as the pour plate method does (20).

Results and discussion

Culturing examination

In the current study, all 50 isolates were cultured on the selective medium CHROMagar, MacConkey agar, and blood agar for colony characterization. They were incubated at 37°C for 24 h. The appearance of *K. pneumonia* colonies on CHROMagar resulted in the formation of mucoid metallic blue colonies, indicating the presence of *K. pneumonia*. (21). On MacConkey agar Pink, mucoid, and lactose fermented colonies were identified as *Klebsiella* spp., however, colonies on blood agar were greyish white, mucoid, and non-hemolytic (22). Bacterial enzymes degraded the artificial chromogenic substrates (chromogens) in the media during metabolism, resulting in the particular coloration of the colonies for each bacterium. These substrates allow

for color-based identification of colonies recovered within 18 to 24 hours of inoculation. The degraded chromogens made it easier to identify mixed growth and enabled better detection rates, The same phenomenon was observed by(23) who went on to say that degraded chromogens would make it easier to identify mixed growth and increase diagnostic accuracy.

Biochemical identification

A variety of biochemical experiments were performed to identify *K. pneumonia*, as shown in Table 1. When a hydrogen peroxides reagent was applied to the colonies, the large majority of the suspected isolates released gas bubbles, suggesting a positive catalase test result. The oxidase test, on the other hand, returned a negative result. All isolates were negative for indole production, motility tests were negative, and the urease test was positive. Lactose fermentation was also detected in the isolates. These traditional biochemical results were compared with the standard result published by (11).

Table (1): Morphological and Biochemical Identification Results of *K. pneumonia*.

No.	Biochemical Test	Result
1	Gram stain	-
2	Catalase production	+
3	Oxidase test	-
4	Indole production	-
5	Urease production	+
6	Lactose fermentation	+
7	Motility test	-
8	Microscopic shape	Road shape

(+): positive; (-): negative

Genotypic identification of *K. pneumonia* isolates

To validate the species identification of *K. pneumonia*, traditional PCR was performed to amplify the *16S rRNA* gene, followed by 1.5 percent agarose gel electrophoresis to confirm the positive result. The genotypic identification of

the *16S rRNA* gene that uses isolates exhibits a 100% positive result with an amplified size of 1410 bp Figure 2. these results were in agreement with (24) who found the isolates of *K. pneumonia* show a similar single band at an approximate 1500 bp size using agarose gel electrophoresis. Thus, the isolates were classified as *Klebsiella*

pneumonia according to amplification of the *16S rRNA* gene.

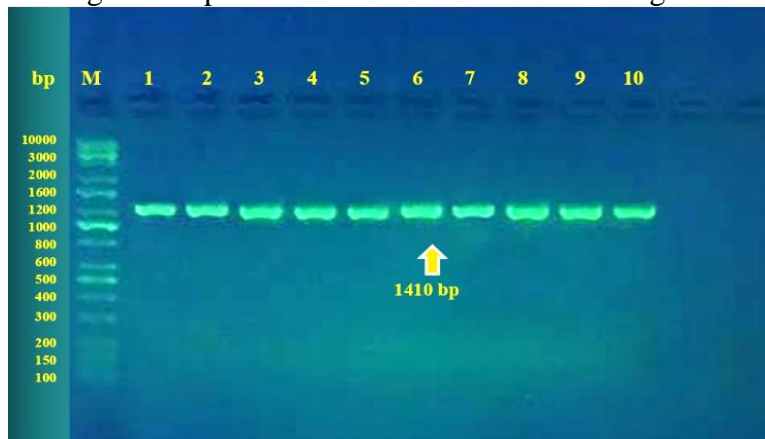


Figure (2): PCR product the band size 1410 bp. The product was electrophoresis on 1.5% agarose at 5 volt/cm². 1x TBE buffer for 1:30 hours. M: DNA ladder (100).

Antibiotic susceptibility assays

The antibiotic susceptibility of *K. pneumoniae* isolates was determined by the disk diffusion method with the guidelines (15). This test was conducted on all 50 isolates against 13 antibiotics. The results revealed that often isolates have a very high level of resistance to the antibiotics used in this study as presented in table 2, which represents Antibiotic susceptibility test results of *K. pneumoniae*, where isolates vary in their susceptibility to the antibiotics. In the present study, most of the isolates were Multi-Drug Resistant (MDR) when tested by the standard disk

diffusion method. These results were in agreement with the results of (25) who find that the majority of *K. pneumoniae* isolates recovered in his study are MDR organisms which limits the available treatment options. Among 50 *K. pneumoniae* isolates tested, 50 isolates 100% were resistant to Trimethoprim and Tetracycline followed by 48 isolates 96% were resistant to Amoxicillin/Clavulanic acid, whereas 22 isolates 44% intermediate to Nitrofurantoin, 42 isolates 84% were sensitive to imipenem and, 38 isolates 76% sensitive to meropenem.

Table (2): Antibiotic susceptibility test results of *K. pneumoniae*.

Antibiotic	Total No. of isolates	No. of R isolates	R	No. of I Isolates	I	No. of S isolates	S
AMC	50	48	96%	0	0%	2	4%
CAZ	50	35	70%	5	10%	10	20%
CIP	50	28	56%	2	4%	20	40%
CN	50	20	40%	0	0%	30	60%
CRO	50	35	70%	0	0%	15	30%
CTX	50	30	60%	10	20%	10	20%
F	50	23	46%	22	44%	5	10%
IPM	50	5	10%	3	6%	42	84%
MEM	50	10	20%	2	4%	38	76%
NA	50	15	30%	7	14%	28	56%
TE	50	50	100%	0	0%	0	0%
TMP	50	50	100%	0	0%	0	0%
TOR	50	15	30%	2	4%	33	66%

R: Resistant, I: Intermediate, S: Sensitive

From the results above *K. pneumonia* develop more resistance to tetracyclines and folate pathway antagonist's class agents with 100% resistance. 96% of isolates resist to β -lactam combination class agents, up to 70% of isolates confer resistance to 3rd generation cephalosporines, and the less resistant was to carbapenems agents with 10%. Nitrofurans class was intermediate activity to *K. pneumonia* with 44% at maximum, and minimum percent of intermediate susceptibility belong to quinolones class, carbapenems class, and aminoglycosides class agents with 4%. The highest sensitivity of *K. pneumonia* isolates was to carbapenems up to 84% these results agreed with the findings of (26) who detected a high level of resistance of 95% among *K. pneumonia* strains to β -lactam combination class agents and, showed high sensitivity to carbapenems class agents, As well as (27) reported the commonest MDR strains were detected from *E.coli*

31.6%, followed by *K. pneumoniae* 30% Raha *et al.* (28) reported the isolates in their study exhibited a low-level resistance against Tigecycline, Meropenem, and Imipenem. Moreover, the relative alteration in the patterns of resistance of *K. pneumoniae* to antibiotics occurs for a variety of reasons, including the size of the studied samples, the varied origin of specimens, site of infection, and predisposition of the patient (29). Furthermore, mutations in plasmid genes that were not previously thought to be resistance genes might play a role in *K. pneumoniae* resistance (30). It is clear from the overall context that *K. pneumoniae* isolates in this study are multi-drug resistant pathogens.

GC-MS analysis

The chemical compositions of *Syzygium aromaticum* extract are determined by GCMS, the retention time and area percent of the composition are listed in Table (3).

Table (3): Chemical composition of *S. aromaticum* Extract

Compound	R. Time	Area%
Eugenol	13.118	77.53
Eugenol	14.148	3.30
Phenol, 2-methoxy-4-(2-propenyl)-acetate	15.860	12.71
Eugenol	16.645	3.54
trans-Isoeugenol	17.193	2.93

The *S. aromaticum* extract contains (84.37%) pure eugenol, according to the results of GC-MS analysis, and three varied retention times of eugenol were discovered. The three approaches' retention times of (13.118), (14.184), and (16.645) minutes, respectively. For eugenol, different retention times have been observed, this result is the same as reported by (31). Eugenol is the major chemical compound in *S. aromaticum* extract, according to the recorded studies, and it has different biological

activities as an antioxidant, anti-carcinogenic, antimicrobial, antifungal, and insecticidal characteristics these results agreed with (32) who founds that the eugenol is the main compound in the *S. aromaticum* extract and has different biological activities.

Characterization of *S. aromaticum* loaded chitosan NPs

Uv-vis spectroscopy

The highest absorbance value at the wavelength 250.00 nm with a value of 1.806 in chitosan NPs loaded *S. aromaticum* extract whereas the highest

value in *S. aromaticum* extract was at a wavelength of 230.00 nm with a value of 1.534, in addition to the disappearance of the wavelength 230.00 nm in the *S. aromaticum* extract and the appearance of a new wavelength at

250.00 in chitosan NPs loaded *S. aromaticum* extract all, indicate the formation of the nanomaterial and the successful loading of the *S. aromaticum* extract on chitosan nanoparticles. Figure (3).

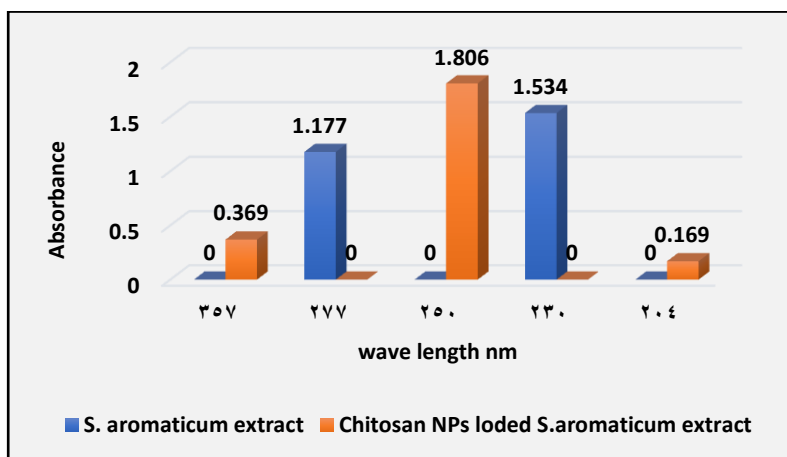


Figure (3): Absorbance difference between *S. aromaticum* extract and chitosan NPs loaded *S. aromaticum* extract by Uv-vis Spectroscopy.

Fourier transformation infrared spectroscopy (FTIR)

In chitosan NPs loaded *S. aromaticum* extract a new spectrum appeared at 449.41 cm^{-1} that was not present in Chitosan, which indicates the emergence of a new bond as a result of the emergence of a new compound. In addition to comparing the spectra area, it was found in Chitosan at the peak 495.71 cm^{-1} , the area was 2.445, while in chitosan NPs loaded *S. aromaticum* extract at the peak 493.78 cm^{-1} the area was 4.326 as well as at the main peak of the Chitosan at 3393.79 cm^{-1}

and its area 86,435 while in chitosan NPs loaded *S. aromaticum* extract the main peak was 3132.4 cm^{-1} and with an area 224,511. this indicates the large molecules were broken into smaller molecules and when they are linked with chitosan, the value of the surface area of the bond increases, and the area increases. Changes in the functional groups of active biomolecules might indicate that they are related to the formation of chitosan NPs loaded *S. aromaticum* extract. Figure (4), these results agree with (33)(34).

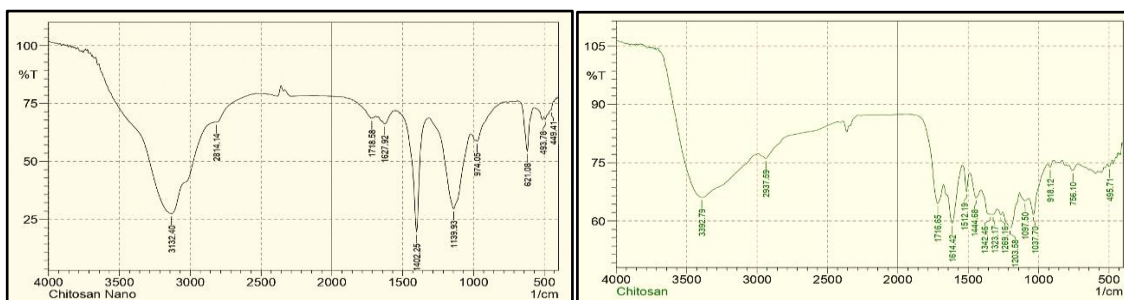


Figure (4): FTIR Spectra Pattern of Chitosan and Chitosan NPs loaded *S. aromaticum* extract

Atomic force microscope analysis AFM

Atomic Force Microscopy images were used to measure particle sizes and the topography of the surface of

Chitosan NPs loaded *S. aromaticum* extract, the size of particles obtained ranged from 26.74 to 53.96 nm Figure (5).

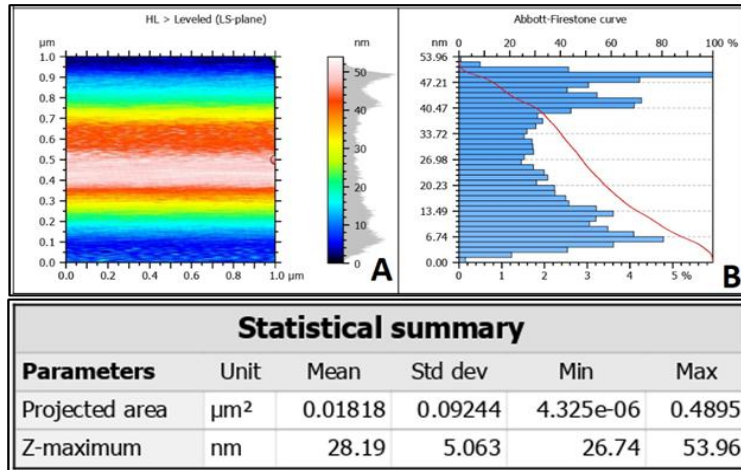


Figure (5): Distribution of Chitosan NPs loaded *S. aromaticum* extract according to particles size

Scanning electron microscope SEM

The morphology of chitosan NPs loaded *S. aromaticum* extract was investigated using SEM, the results were presented in Figure (6) chitosan

NPs loaded *S. aromaticum* extract have a spherical appearance with a diameter range 37.96-79.01 nm. and have a relatively homogeneous morphology.

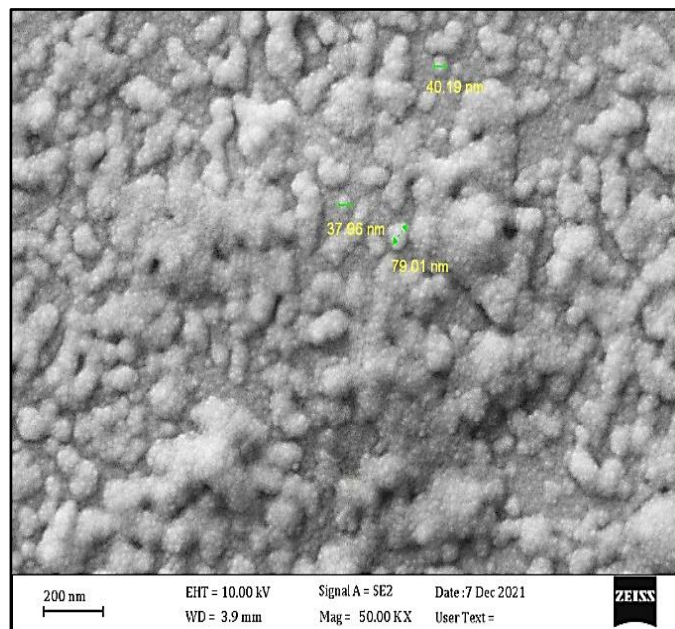


Figure (6): Scanning Electron Microscopy image of chitosan NPs loaded *S. aromaticum* extract

X-ray diffraction XRD

Figure (7A) shows the X-ray diffraction patterns of chitosan. Which shows the main peak of 2θ value at 20.53° and an intensity level close to 1200 cont. On the other hand, Figure (7B) shows the chitosan NPs loaded *S. aromaticum* extract peak, which shows

its main peak of 2θ value at 22.8596° and an intensity level at 736.5503 cont. this change indicates the difference in the crystal structure between these two materials where chitosan NPs loaded *S. aromaticum* extract were more crystalline than Chitosan.

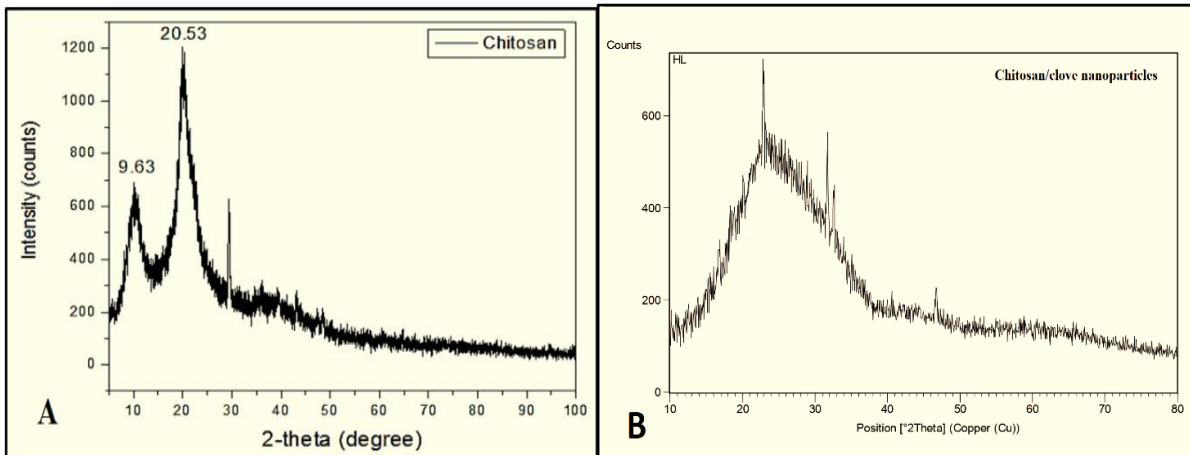


Figure (7) (A) Diffractogram of Chitosan (35), (B) Diffractogram of chitosan NPs loaded *S. aromaticum* extract

Antibacterial activity of chitosan NPs loaded *S. aromaticum* extract

The spread plate method SPM was used to evaluate the antimicrobial activity of chitosan NPs loaded *S.*

aromaticum extract against *K. pneumonia* isolates that showed the highest rate of antibiotic resistance (36). The results are listed in the table (4).

Table (4): The antibacterial activity of different concentrations of Chitosan NPs loaded *S. aromaticum* extract against *K. pneumonia*.

Isolates	Chitosan NPs loaded <i>Syzygium aromaticum</i> Extract concentrations							LSD
	100%	50%	25%	12.5%	6.25%	3.12%	Control	
K33	0	0	0	0	0	100	1.5*10 ⁸	0.0001**
K35	0	0	0	0	2	1600	1.5*10 ⁸	0.0001**
K36	0	0	0	0	0	0	1.5*10 ⁸	0.0001**
K37	0	0	0	0	3	900	1.5*10 ⁸	0.0001**
K40	0	0	0	0	0	300	1.5*10 ⁸	0.0001**
K41	0	0	0	0	5	1100	1.5*10 ⁸	0.0001**
K42	0	0	0	0	8	760	1.5*10 ⁸	0.0001**
K46	0	0	0	0	3	1400	1.5*10 ⁸	0.0001**
K47	0	0	0	0	5	860	1.5*10 ⁸	0.0001**
K50	0	0	0	0	0	120	1.5*10 ⁸	0.0001**
P-value	0.0001**							----
P≤0.01**								

From the results above, it was observed that there was an inhibitory effect of Chitosan NPs loaded *S. aromaticum* Extract against bacterial growth, the highest inhibition activity was at a concentration of 100%, 50%, 25%, and 12.5%, as no growth of bacterial colonies was observed, and the result was zero colonies for all isolates compared with the control of each isolate which was 1.5×10^8 CFU/ml. In the concentration of 6.25 %, there are a few colonies were observed, and the highest growth was 8 CFU/ml in the isolate K42 and the other growth ranged from 2 to 5 CFU/ml for other isolates besides the isolates K33, K36, K40, and K50 was no growth while its control was 1.5×10^8 CFU/ml. However, for the concentration of 3.12 %, there is a growth in most of the isolates ranging from 100 to 2000 CFU/ml while the isolate K36 was no growth while its control was 1.5×10^8 CFU/ml. The results were statistically analyzed and showed high significant differences compared with control at probability ($P \leq 0.01$). These results approved that the Chitosan NPs loaded *S. aromaticum* Extract have antibacterial activity against *K. pneumonia* isolates with different concentrations these findings were agreed with (37) (38) who founds that Chitosan NPs have a wide spectrum of antimicrobial activity against different pathogenic bacteria. As well as (39) reported that the key finding of his work is that chitosan-alginate NPs are effective for treating Enterobacteriaceae infections. The role of plant extract loaded with the NPs that the Plant extracts work as both reducing and stabilizing agents. Phenolic and flavonoid chemicals act as reducing agents, whereas amino acids function as stabilizing agents. Which increases the activity and stability of nanoparticles (40). The results admit with (41) who

revealed that chitosan nanoparticles synthesized by the ionic gelation method possess strong antibacterial activity against Gram-negative bacteria. The electrostatic force between the Chitosan NPs loaded *S. aromaticum* Extract and the bacterium cell wall promotes a tighter contact with charged molecules, allowing NPs to pass through the cell wall. Furthermore, Chitosan NPs loaded *S. aromaticum* Extract can alter the electron transport chain of bacteria (42). Electrostatic interactions, which alter membrane permeability, are the most commonly suggested antibacterial activity of Chitosan NPs loaded *S. aromaticum* Extract. It then attaches to DNA, preventing DNA replication and ultimately causing bacterial cell death(43,44,45).

Conclusion

The present study concluded that Chitosan NPs loaded with *Syzygium aromaticum* Extract has antibacterial activity against *K. pneumonia* strains that have resistance to antibiotics, Considering the effectiveness of plant extracts on multi-drug resistant bacteria *in vitro*, we recommend more research on these extracts *in vivo* as therapeutic alternatives, especially after loading on nanomaterials, because this increases their antibacterial activity in small quantities, safe and economic value.

References

1. Khan, I., K. and Khan, I. (2019). Nanoparticles: Properties, applications, and toxicities of *Syzygium aromaticum* Extracted. Arabian Journal of Chemistry, 12(7):908–931.
2. Kaushal, S. and Kaur, K. (2019). Phytochemistry and pharmacological aspects of *Syzygium aromaticum*: A review K Kaur and S Kaushal. Journal of Pharmacognosy and Phytochemistry, 8(1):398-406.
3. Neveu, V.; Perez-Jiménez, J.; Vos, F.; Crespy, V.; Chaffaut, L. and Mennen, L. (2010). An online comprehensive database on polyphenol contents in foods. Database:

- The Journal of Biological Databases and Curation, online.
4. Rai, M. and Yadav, A. (2013). Plants as potential synthesiser of precious metal nanoparticles: Progress and prospects. *IET Nanobiotechnology*,7(3):17–24.
 5. Antunes, J.; Domingues, J.; Miranda, C.; Silva, A.; Homem, N. and Amorim, M. (2021) Bioactivity of chitosan-based particles loaded with plant-derived extracts for biomedical applications: Emphasis on antimicrobial fiber-based systems. *Marine Drugs*,19(7):2-40.
 6. Upadhyay, R.; Shenoy, L. and Venkateswaran, R. (2018). Effect of intravenous dexmedetomidine administered as bolus or as bolus-plus-infusion on subarachnoid anesthesia with hyperbaric bupivacaine. *Journal of Anaesthesiology Clinical Pharmacology*,34(3):46–50.
 7. Alqahtani, F.; Aleanizy, F.; Tahir. E.; Alhabib, H.; Alsaif, R. and Shazly, G. (2020). Antibacterial activity of chitosan nanoparticles against pathogenic n. *Gonorrhoea*. *International Journal of Nanomedicine*,15:7877–7887.
 8. Miller, M. and Zachary, J. (2017). Mechanisms and Morphology of Cellular Injury, Adaptation, and Death1. *Pathologic Basis of Veterinary Disease*, e19:2-43.
 9. Holt, K.; Zhou, H.; Bachman. M. and Martin. R. (2018) Colonization, Infection, and the Accessory Genome of *Klebsiella pneumoniae*. *Frontiers in Cellular and Infection Microbiology*,8(4)1-15.
 10. Brooker, C. (2008). *Churchill Livingstone Medical Dictionary*. Elsevier Health Sciences.
 11. Mac Faddin, J. (2000). *Biochemical tests for identification of medical bacteria*. Philadelphia: Lippincott Williams & Wilkins.
 12. Collee, M.; McCartney, J. (1996). Mackie and McCartney practical medical microbiology. New York: Churchill Livingstone.
 13. Srinivasan, R.; Karaoz, U.; Volegova, M. MacKichan, J.; KatoMaeda, M. and Miller, S. (2015). Use of 16S rRNA gene for identification of a broad range of clinically relevant bacterial pathogens. *PLoS One*,10(2):1–22.
 14. Sambrook, J.; Roberts, K.; Walter, P. and Green, M. (2015). *Molecular Cloning A Laboratory Manual Fourth Edition*.
 15. Wayne, P. (2021). *Performance Standards for Antimicrobial Susceptibility Testing*. 31st ed. Clinical and Laboratory Standards Institute, 1–315 p.
 16. Sultana, B.; Anwar, F. and Ashraf, M. (2009). Effect of extraction solvent/technique on the antioxidant activity of selected medicinal plant extracts. *Molecules*, 14(6):2167–180.
 17. Amelia, B.; Extractpudin, E.; Cahyana, A.; Rahayu, D.; Sulistyoningrum, A. and Haib, J. (2017). GC-MS analysis of clove (*Syzygium aromaticum*) bud essential oil from Java and Manado. *ConferenceProceeding*,1862(7):1-9.
 18. El-Ghaffar, M.; Hashem, M. (2010). Chitosan and its amino acids condensation adducts as reactive natural polymer supports for cellulase immobilization. *Carbohydrate Polymers*. 81(3):507–516.
 19. Nasti, A.; Zaki, N.; DeLeonardis, P.; Ungphaiboon, S. Sansongsak, P. and Rimoli, M. (2009). Chitosan/TPP and chitosan/TPP-hyaluronic acid nanoparticles: Systematic optimisation of the preparative process and preliminary biological evaluation. *Carbohydrate Polymers*, 26(8):1918–1930.
 20. Wise, K. (2006). *Preparing Spread Plates Protocols*. American Society for Microbiology Microbe Library, 1–8.
 21. Samra, Z.; Heifetz, M.; Talmor, J.; Bain, E. and Bahar, J. (1998). Evaluation of use of a new chromogenic agar in detection of urinary tract pathogens. *Journal of Clinical Microbiology*, 36(4):990–94.
 22. Klaif, S.; Nasir, H. and Sadeq, J. (2018). The genetic relationship for *klebsiella pneumoniae* isolated from human urinary tract and beef. *Iraqi Journal of Veterinary Sciences*,33(1):75–80.
 23. Abdul Redha, A. and RSSA, J. (2017). Characterization of Biofilm Production in Antibiotic Resistant *Klebsiella Pneumonia* Isolated from Different Clinical Samples in Iraqi Hospitals. *Journal of Global Pharma Technology*, 2(9):26–34.
 24. Budiarso, T.; Amarantini, C. and Pakpahan, S. (2021). Biochemical identification and molecular characterization of *klebsiella pneumoniae* isolated from street foods and drinks in yogyakarta, indonesia using 16s rRNA gene. *Biodiversitas*, 22(12):5452–5458.
 25. Bobbadi, S.; Chinnam, B.; Reddy, P. and Kandhan, S. (2021). Analysis of antibiotic resistance and virulence patterns in *Klebsiella pneumoniae* isolated from human urinary tract infections in India. *Letters in Applied Microbiology*,73(5):590–598.

26. Abdullah, F.; Mushtaq, A.; Irshad, M.; Rauf, H.; Afzal, N. and Rasheed, A. (2013). Current efficacy of antibiotics against *Klebsiella* isolates from urine samples - A multi-centric experience in Karachi. *Pakistan Journal of Pharmaceutical Sciences*, 26(1):11–15.
27. Basak, S.; Singh, P. and Rajurkar, M. (2016). Multidrug Resistant and Extensively Drug Resistant Bacteria: A Study *Journal of Pathogens*:1–5.
28. Rahal, B.; Abdulhassan, A.; Salman, N. and Kassim, K. (2021). The Role of EDTA in Biofilm Eradication of *Klebsiella pneumoniae* Isolated from Wound Infections. *Iraqi Journal of Biotechnology*, 20(1):96–102.
29. Paczosa, M. and Meccas, J. (2016). *Klebsiella pneumoniae*: Going on the Offense with a Strong Defense, *Microbiology and Molecular Biology Reviews*, p. 629–661.
30. Bernardini, A.; Cuesta, T.; Tomás, A.; Bengoechea, JA.; Martínez, JL. and Sánchez, MB. (2019). The intrinsic resistome of *Klebsiella pneumoniae*. *International Journal of Antimicrobe Agents*, 53(1):29–33.
31. Purwanti, N.; Zehn, A.; Pusfitasari, E.; Khalid, N.; Febrianto, E. and Mardjan, S. (2018). Emulsion stability of clove oil in chitosan and sodium alginate matrix. *International Journal of Food Properties*, 21(1):566–581.
32. Javed, R.; Zia, M.; Naz, S.; Aisida, S.; Ao, Q. (2020). Role of capping agents in the application of nanoparticles in biomedicine and environmental remediation: recent trends and future prospects. *Journal of Nanobiotechnology*, 18(1):1–15.
33. Agarwal, M.; Agarwal, MK.; Shrivastav, N.; Pandey, S.; Das, R. and Gaur, P. (2018). Preparation of Chitosan Nanoparticles and their In-vitro Characterization. *International Journal of Life-Sciences*, 4(2):1713–1720.
34. Almukhtar, JG. and Karam, FF. (2020). Preparation characterization and application of Chitosan nanoparticles as drug carrier *Journal of Physics Conference Series*, 1664(1).
35. Chandra, S.; Al – Amin, M.; Ur Rashid, T.; Zakir, M.; Ashaduzzaman, M. and Sarker, M. (2016). Preparation, Characterization and Performance Evaluation of Chitosan as an Adsorbent for Remazol Red. *International Journal of Latest Research in Engineering and Technology*, 2016, 52–62.
36. Tamara, F.; Lin, C. Mi, F. and Ho, Y. (2018). Antibacterial effects of chitosan/cationic peptide nanoparticles. *Nanomaterials*, 8(2):1–15.
37. Jampilek, J. and Kralova, K. (2022). Advances in Nanostructures for Antimicrobial Therapy. *Materials*, 15(7):2388.
38. Wei, D.; Sun, W.; Qian, W.; Ye, Y. and Ma, X. (2009). The synthesis of chitosan-based silver nanoparticles and their antibacterial activity. *Carbohydrate Research*, 344(17):2375–2382.
39. Kadhum, W. and Zaidan, I. (2020). The Synergistic Effects of Chitosan-Alginate Nanoparticles Loaded with Doxycycline Antibiotic Against Multidrug Resistant *Proteus Mirabilis*, *Escherichia Coli* and *Enterococcus Faecalis*, *Iraqi Journal of Science*, 61(12):3187–3199.
40. Rabia, J.; Usman, M. and MZ. (2016). Effect of capping agents: Structural, optical and biological properties of ZnO nanoparticles *Applied Surface Science*, 386, 319–326.
41. Hipalawins, W.; Balakumaran, M.; Jagadeeswari, S. (2016). Synthesis, Characterization, and Antibacterial Activity of Chitosan Nanoparticles and their Impact on Seed Germination. *Journal of Academia and Industrial Research*, 5(5):65.
42. Ivask, A.; Elbadawy, A.; Kaweeteerawat, C.; Boren, D.; Fischer, H. and Ji, Z. (2014). Toxicity mechanisms in *Escherichia coli* vary for silver nanoparticles and differ from ionic silver. *ACS Nano*, 8(1):374–386.
43. Birsoy, K.; Wang, T. and Chen, W. (2015). An Essential Role of the Mitochondrial Electron Transport Chain in Cell Proliferation Is to Enable Aspartate Synthesis. *Cell*, 162(3):540–551.
44. Al-Ahmer, S. D., Shami, A. M., and Al-Saadi, B. Q. H. (2018). Using of Hybrid Nanoantibiotics as Promising Antimicrobial Agent. *Iraqi Journal of Biotechnology*, 17(3):1–12.
45. Tawfeeq, A. T. (2013). Pulsed laser ablation synthesized silver nanoparticles induce apoptosis in human glioblastoma cell line and possess minimal defect in mice brains. *Iraqi Journal of Biotechnology*, 12(2), 92–106.